

Accommodate Knowledge Conflicts in Retrieval-augmented LLMs: Towards Robust Response Generation in the Wild

Jiatai Wang^{1,2}, Zhiwei Xu^{2,3*}, Di Jin⁵, Xuewen Yang⁴, Tao Li^{1,2,*}

¹The College of Computer Science, Nankai University, Tianjin, China

²Haihe Lab of ITAI, Tianjin, China

³Institute of Computing Technology, Chinese Academy of Sciences, Beijing, China

⁴The Department of Electrical and Computer Engineering, Stony Brook University, New York, U.S.A

⁵Eigen AI, Palo Alto, U.S.A

1120240357@mail.nankai.edu.cn, xuzhiwei2001@ict.ac.cn, di@eigenai.com, michelyang1990@gmail.com, litao@nankai.edu.cn

Abstract

The proliferation of large language models (LLMs) has significantly advanced intelligent systems. Unfortunately, LLMs often face knowledge conflicts between internal memory and retrieved external information, arising from misinformation, biases, or outdated knowledge. These conflicts undermine response reliability and introduce uncertainty in decision-making. In this work, we analyze how LLMs navigate knowledge conflicts from an information-theoretic perspective and reveal that when conflicting and supplementary information exhibit significant differences, LLMs confidently resolve their preferences and alleviate the uncertainty during their response generation. When this difference is ambiguous, LLMs experience considerable uncertainty about their generation. Based on this insight, we propose Swin-VIB, a novel framework that integrates a pipeline of variational information bottleneck models to adapt the retrieved information difference, facilitating robust response generation of LLMs even in conflicting contexts. Extensive experiments confirm our theoretical analysis and demonstrate the performance of Swin-VIB. Notably, Swin-VIB outperforms all competitive baselines in terms of the accuracy of the multiple-choice task, while improving the EM values in the open-ended QA task by at least 11.14%.

1 Introduction

As large language models (LLMs) (Brown et al. 2020; OpenAI 2023) continue to proliferate, their powerful generation capabilities facilitate more transformative technologies for advanced intelligent systems. Among these novel technologies, despite the response generation technique (Li et al. 2024) allows LLMs to answer queries without rigid retrieval, it still suffers from hallucinations. Augmented LLMs with external knowledge, including retrieval augmented generation (RAG), have become a promising solution to mitigating these issues (Lewis et al. 2020; Gao et al. 2023; Asai et al. 2023). However, the disparity between the internal memory of LLM and the retrieved external context always leads to knowledge conflicts (Xu et al. 2024). These conflicts arise from misinformation, unreliable sources, and publisher bias in retrieved information, and the difficulty in synchronizing

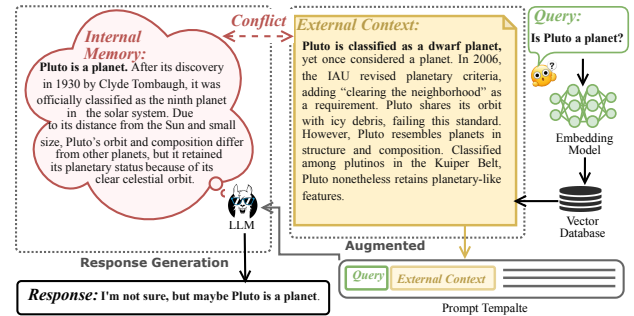


Figure 1: Illustration of knowledge conflict in RAG.

parametric knowledge with the context in real time further exacerbates these conflicts. As illustrated in Figure 1, these conflicts introduce uncertainty in response generation (Wu, Wu, and Zou 2024), posing a serious threat to the reliability of the responses and increasing the risk of biased or erroneous inference.

The existing approaches do not fully agree on how LLMs resolve knowledge conflicts. Some works prefer to fine-tune or edit LLMs according to external context and guiding response generation. (Shi et al. 2023b; Jin et al. 2024b; Zhang, Yu, and Feng 2024). In contrast, others attach external-validation modules that merely admit trusted context to supplement the internal memory of LLMs (Yu, Zhang, and Feng 2024; Kortukov et al. 2024). However, both of them have a fixed preference for the used knowledge that is often violated. This contradiction exposes a fundamental dilemma that without a principled framework explaining how such preferences emerge, either fine-tuning or external-validation modules risks the wrong optimizing results. Although new efforts try to re-balance internal memory and external context during model decoding (Shi et al. 2023a; Jin et al. 2024a; Huang et al. 2025), their token-level weight updating fails to scale to mitigate fundamental knowledge conflicts in practice. Therefore, a theoretical analysis of the knowledge preference and uncertainty is highly desired to extend the existing heuristic guidelines toward knowledge conflicts mitigation and robust response generation.

*Corresponding authors

To address this challenge, we re-examine knowledge conflict in response generation from the perspective of information theory. We analyze how LLMs establish preferences on the information used to generate responses when faced with conflicting knowledge sources and observe:

- When the disparity between conflicting and supplementary information is significant, LLMs confidently settle into a rational knowledge preference and generate reliable responses.
- When the distinction is ambiguous, LLMs experience extreme uncertainty, making their response unreliable.

Inspired by these insights, we propose Swin-VIB, a Variational Information Bottleneck (VIB) approach with a Sliding window. More specifically, we leverage a pipeline-based multiple variational information bottleneck models (Alemi et al. 2016) to augment the retrieved information adaptively and guide the preference of LLMs. This design adapts the LLM’s preference and minimizes ambiguity, enabling more accurate and consistent response generation even in challenging scenarios with knowledge conflicts. Swin-VIB can be plugged into RAG pipelines almost without any additional overhead. Our major contributions are summarized as follows:

- We model the interplay between LLMs’ internal memory and external context and release the preference principle behind knowledge conflict in retrieval-augmented LLMs. With significant differences between conflicting and supplementary information, LLMs have more confidence to settle into a rational preference; otherwise, LLMs fall into extremely high uncertainty.
- This analysis of LLMs’ preference provides insight into accommodating knowledge conflicts in retrieval-augmented LLMs. In this way, we propose Swin-VIB¹, a sliding-window approach that integrates multiple variational information bottlenecks to adapt perplexing knowledge, enhancing it to guide LLMs toward accurate responses.
- Extensive experiments across multiple-choice and open-ended question answering (QA) validate our theoretical result and demonstrate that Swin-VIB outperforms baselines for robust response generation in the wild.

To the best of our knowledge, this is the first approach that analyzes and evaluates knowledge conflicts of retrieval-augmented LLMs. A robust response generation paradigm is proposed according to the obtained insight, rather than merely relying on empirical evaluations, thus enjoying enhanced performance.

2 Preliminary

2.1 Definitions

Knowledge conflicts may cause uncertainty in response generation, where LLMs need to make a choice with conflicting knowledge from their internal memory and the external context. Considering the black-box nature of LLMs, it remains challenging to analyze the fundamental mechanism of these conflicts between invisible internal knowledge and external

¹The code is available at <https://github.com/JiataiWang/Swin-VIB>.

contexts. Without a theoretical analysis of knowledge conflicts, the limitations of empirical rules and experimental settings in response generation can hardly alleviate knowledge conflicts (Wu, Wu, and Zou 2024; Xie et al. 2023; Jin et al. 2024a). To tackle this challenge, we propose a theoretical framework that shows knowledge conflicts can be defined in terms of conditional entropy. The corresponding symbol system is outlined in Table 1.

Symbol	Meaning
Q	Queries
$R = B(Q)$	External contexts from the knowledge base B
$O = \text{LLM}(R, Q)$	Responses generated by the LLM

Table 1: A list of Symbols

Definition 1 (Uncertainty of response generation).

The uncertainty of O given the Q and R is represented by conditional entropy \mathbb{H} , is formalized by

$$\mathbb{H}(O | R, Q) = - \sum_{o \in O, r \in R, q \in Q} p(o, r, q) \log p(o | r, q), \quad (1)$$

A commonsense assumption is taken to regulate the RAG process.

Assumption 1 (Non-void Retrieval). A qualified external information retriever can recall external contexts correlated with the corresponding query (Robertson and Jones 1976), that is $\forall q \in Q, \exists r \in R, p(r, q) > 0$, where q is a query, and r is one correlated external context.

2.2 Theoretical Analysis

We reveal how the difference between conflicting and supplementary information influences the reliability of LLMs. A brief analysis is listed as follows, and all details about this analysis are provided in Appendix A.

Step 1: Uncertainty formulation. According to Definition 1 and Assumption 1, we rewrite Formula 1 based on the law of total probability and the chain rule (see Appendix A.1):

$$\mathbb{H}(O | R, Q) = \sum_q p(q) \sum_r p(r | q) \sum_o \psi(p(o | r, q)), \quad (2)$$

where $\psi(\cdot)$ denotes instance-level uncertainty, and is calculated by

$$\psi(p(o | r, q)) = -p(o | r, q) \log p(o | r, q) \quad (3)$$

Step 2: Latent-state decomposition. Let X be the high-dimensional latent space of the LLM, and let $x \in X$ denotes a specific latent state activated during generation (see Appendix

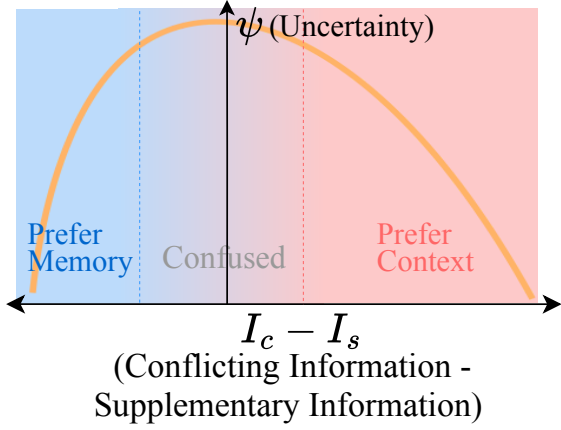


Figure 2: Relationship between uncertainty and the information difference.

A.2). We have:

$$\begin{aligned}
p(o | r, q) &= \int_X p(o | r, q, x) p(x | r, q) dx \\
&= \int_X p(o | r, q, x) \frac{p(r, q | x) p(x)}{p(r, q)} dx \\
&\propto \int_X p(o | r, q, x) p(r, q | x) p(x) dx \\
&\propto \int_X p(o | r, q, x) \frac{p(r, q | x)}{p(r, q | x_\gamma)} p(x) dx \\
&\approx \int_X p(o | r, q, x) \exp[\log p(r | x) - \log p(r | x_\gamma)] p(x) dx \\
&\propto \int_X p(o | r, q, x) \exp[I_c - I_s] p(x) dx,
\end{aligned} \tag{4}$$

where self-information $I_s = -\log p(r | x)$ denotes the external information consistent with the LLM’s memory, namely, supplementary information, whereas $I_c = -\log p(r | x_\gamma)$ denotes the information that contradicts internal memory and is defined as conflicting information, with $x_\gamma \in X$ being a latent state aligned to the retrieved context r .

Step 3: Approximation Leveraging the monotonicity of $\exp(\cdot)$, and the constants are reduced after normalizing $p(o | r, q)$ over o , we apply a Taylor expansion and arrive at the following approximation (see Appendix A.3):

$$p(o | r, q) \propto I_c - I_s. \tag{5}$$

Equation (5) is a first-order proxy of the exponential, and monotonic claims in Step 4 rely only on the monotonicity of the exponential tilt (proved in Appendix A.3).

Step 4: Theoretical statement. According to Formula (5), Formula (3) reveals a relation between uncertainty ψ and the information difference $\Delta I = I_c - I_s$. Larger $|\Delta I|$ consistently corresponds to lower ψ , i.e. $|\Delta I| \uparrow \iff \psi \downarrow$, which can also be found in Figure 2. Equivalently, the conditional entropy is the weighted expectation of instance-level uncer-

tainty,

$$\mathbb{H}(O | R, Q) = \mathbb{E}_{q \sim p(q)} \mathbb{E}_{r \sim p(r|q)} \left[\sum_o \psi(p(o | r, q)) \right], \tag{6}$$

So lowering the per (q, r) uncertainty in expectation lowers $\mathbb{H}(O | R, Q)$. The full derivation can be found in Appendix A.4.

3 Methodology

According to our theoretical analysis, a larger information difference $|\Delta I|$ of conflicting and supplementary information enhances response reliability, and thus we take this insight to design Swin-VIB, which integrates a pipeline of variational information bottleneck models to adapt the external information in those context windows with large $|\Delta I|$.

3.1 Overview

To maximize the information difference between conflicting and supplementary information in the external context, the retrieved context is first segmented into fixed-length windows to give a unified unit on which the information difference is measured. Specifically, Swin-VIB slides over these windows and quickly predicts the difference in information contained in each window. The window with a large enough information difference is accepted; otherwise, the window is rejected. Finally, Swin-VIB concatenates the accepted windows with the query to form a prompt, as shown in Figure 3.

3.2 Data Preparation

Given a dataset $\mathcal{D} = \{(q, r)\}$, where each query q is paired with an external context $r \in \{r_c, r_s, r_m\}$, r_c is conflicting context, r_s is supplementary context, and r_m is their mixture. To construct the mixed context r_m , conflicting and supplementary contexts interleave each other by every 4 tokens, eliminating the possibility of sampling a window only with conflicting context or supplementary context. For each query q , we randomly extract a fixed-length window of length 7 from the context r .

$$\omega^* \leftarrow \text{RandomWindow}(r, \text{len} = 7), \tag{7}$$

and for this window, a binary label is assigned as

$$\mathbf{Y} = \begin{cases} 1, & \text{if } r \text{ is from single source, } r \in \{r_c, r_s\} \\ 0, & \text{if } r \text{ has multiple sources, } r = r_m \end{cases} \tag{8}$$

This setting guarantees \mathbf{Y} represents the information difference $|\Delta I|$. Because $r \in \{r_c, r_s\}$ denotes all tokens originate from a single source, the ω^* carries a maximal difference between conflicting and supplementary information. If $r \in \{r_m\}$, the ω^* inevitably contains multiple optional instances from different sources and therefore exhibits a small information difference, matching the multiple optional condition.

Feeding each ω^* into a frozen LLM yields a stack of per-layer attention matrices $\{\mathbf{A}_n\}$. We average heads to obtain

$$\mathbf{G}_n = \text{MEANHEADS}(\mathbf{A}_n), \tag{9}$$

and construct the training set

$$T_n = \{\mathbf{G}_n, \mathbf{Y}\}^N \tag{10}$$

All \mathbf{G}_n of LLM decoder layers share the same \mathbf{Y} . Detailed in Algorithm 1.

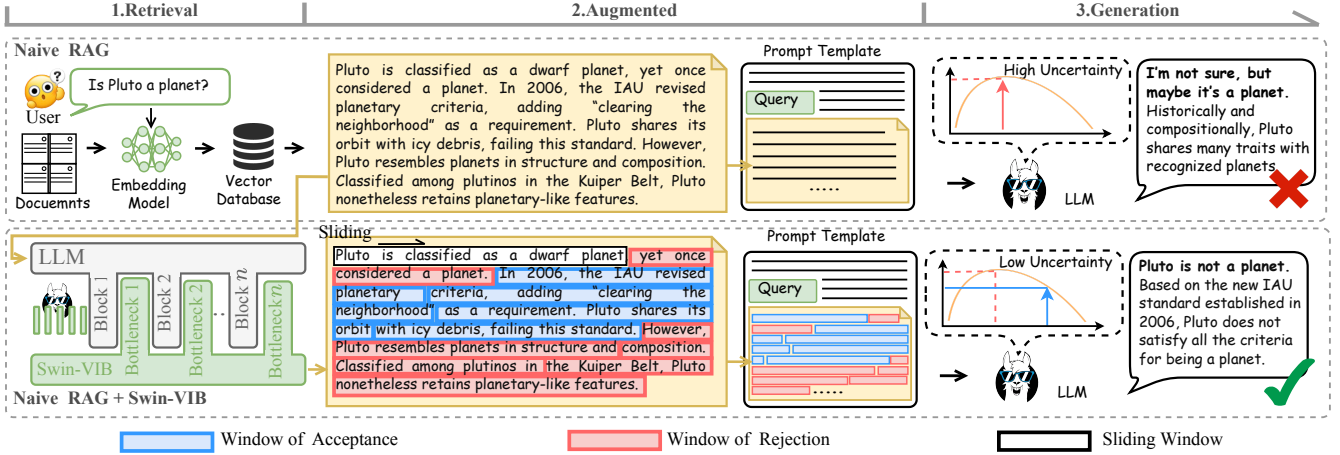


Figure 3: An overview of response generation with Swin-VIB.

Algorithm 1: Training-Set Construction

Input: Dataset \mathcal{D} ; LLM \mathcal{M} with N layers
Output: Training sets $T_n = (\mathbf{G}, \mathbf{Y})_{n=1}^N$

- 1 Initialise $T_n \leftarrow []$ for $n = 1, \dots, N$;
- 2 **for** each sample $\{q, r\} \in \mathcal{D}$ **do**
- 3 $\omega^* \leftarrow \text{RandomWindow}(r, \text{len})$;
- 4 $\mathbf{Y} \leftarrow \begin{cases} 1, & \text{if } r \in \{r_c, r_s\}, \\ 0, & \text{if } r = r_m \end{cases}$;
- 5 **for** $n \leftarrow 1$ **to** N **do**
- 6 $\mathbf{A}^{(n)} \leftarrow \text{Attention}(\omega^*, n)$;
- 7 $\mathbf{G}_n \leftarrow \text{MeanHeads}(\mathbf{A}_n)$;
- 8 **append** (\mathbf{G}_n, Y) to T_n ;
- 9 **return** $\{T_n\}_{n=1}^N$; // each saved via pickle.dump

3.3 Swin-VIB Architecture & Training

We propose a novel method Swin-VIB to compress various information and extract their differences adaptively. Inspired by the information bottleneck structure (Tishby, Pereira, and Bialek 2000), Swin-VIB introduces an information bottleneck into each transformer decoder layer to predict the information difference of the external context. In the following, we describe how the constructed training sets T_n are fed into these bottlenecks for training.

As shown in Figure 4, a bottleneck model consists of an encoder and a decoder, the encoder projects \mathbf{G}_n of an LLM layer to the mean μ_n and log-variance $\log \sigma_n^2$ of each Gaussian latent feature.

$$q_\theta(\mathbf{Z}_n | \mathbf{G}_n) = \mathcal{N}(\mu_n, \text{diag}(\sigma_n^2)). \quad (11)$$

where θ and ϕ are the parameters of the encoder and the decoder. Via the reparameterization trick (Kingma and Welling 2013), we obtain a differentiable latent representation,

$$\mathbf{Z}_n = \mu_n + \sigma_n \odot \epsilon, \quad \epsilon \sim \mathcal{N}(\mathbf{0}, \mathbf{I}). \quad (12)$$

The decoder maps \mathbf{Z}_n to the logit of $\hat{Y}_n = p_\phi(Y = 1 | \mathbf{Z}_n)$, and predicts whether a window includes a larger informa-

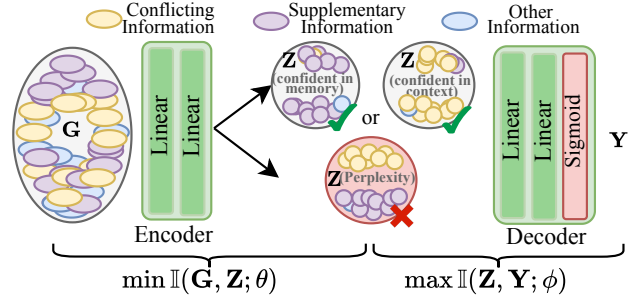


Figure 4: Bottleneck model structure and training objective.

tion difference. Each bottleneck is trained independently by minimizing the information bottleneck loss:

$$\mathcal{L}_n(\theta, \phi) = \underbrace{\mathbb{E}_{q_\theta}[-\log p_\phi(Y | \mathbf{Z}_n)]}_{\uparrow \mathbb{I}(\mathbf{Z}_n; Y)} + \underbrace{\beta \text{KL}(q_\theta(\mathbf{Z}_n | \mathbf{G}_n) | p(\mathbf{Z}))}_{\downarrow \mathbb{I}(\mathbf{G}_n; \mathbf{Z}_n)} \quad (13)$$

where $p(\mathbf{Z}) = \mathcal{N}(\mathbf{0}, \mathbf{I})$ is an isotropic prior and parameter β controls the compression–prediction trade-off. It is by minimizing the mutual information $\mathbb{I}(\mathbf{G}, \mathbf{Z})$ to guide the encoder to adaptively learn the key features to identify information differences. The KL term upper-bounds $\mathbb{I}(\mathbf{G}_n; \mathbf{Z}_n)$, and thus makes the encoder discard redundant information.

3.4 Robust Response Generation

To achieve robust response generation, we incorporate the corresponding bottleneck into the inference process of each transformer-decoder layer of LLM. More specifically, the RAG retriever recalls an external context r , which is partitioned into fixed-length windows $r = \{\omega^1, \dots, \omega^K\}$. Each window ω^k is fed to the frozen LLM to get attention representation \mathbf{G}_n^k , which is collected from every decoder layer. The representation is fed into the corresponding layer-specific

bottleneck model, where the encoder’s mean μ is efficiently taken as the latent \mathbf{Z}_n to skip sampling. The bottleneck returns a layer-wise probability $p_{\phi_n}(Y=1 | \mathbf{G}_n^k)$ that predicts the information difference in terms of different context windows. The outputs of all bottlenecks are weighted to achieve an averaging result to guide robust response generation:

$$\hat{p}(q, \omega^k) = \frac{1}{N} \sum_{n=1}^N p_{\phi_n}(Y=1 | \mathbf{G}_n^k), \quad (14)$$

A window is accepted if $\hat{p}(\omega^k) \geq \xi$, where ξ is a threshold. All accepted windows are concatenated with the query to construct the final prompt $[q; \{\omega^k | \hat{p}(\omega^k) \geq \xi\}]$. In this way, the LLM is guided to generate reliable responses, even in the case that the context contains a large amount of conflicting information.

4 Experiments

In this section, we verify our theoretical analysis and demonstrate that Swin-VIB can reliably guide LLMs to adapt to conflicting external context and generate the correct responses.

4.1 Experimental Settings

Datasets We use three popular datasets to evaluate the performance of Swin-VIB. Note that these datasets contain supplementary contexts and conflicting contexts, but don’t have any mixed contexts.

- ConflictQA (Xie et al. 2023) (2,839 samples): Each q contains internal knowledge "parametric memory" and conflicting external context "counter memory", mapping them to r_s and r_c , respectively.
- DRUID (Hagström et al. 2024) (1,003 samples): Each q contains a two-option item with mutually exclusive claim A/B (each paired with supporting evidence); the verified claim becomes r_s , the refuted one r_c .
- TruthfulQA (Lin, Hilton, and Evans 2021) (817 samples): Each q has one best-answer candidate which serves as the ground truth, multiple other correct responses, and a collection of incorrect alternatives. We use LLMs to select among the above options as r_s , unselected options are r_c .

Our construction only requires including queries paired with contexts from different sources. Specifically, given a query q , the LLM first answers, the chosen option is treated as supplementary to its internal memory, and the unchosen option as conflicting. For LLMs not covered by the original dataset, we follow the two-step procedure: (i) obtain a closed-book answer and rationale as Internal Memory; (ii) prompt ChatGPT to draft a coherent passage that contradicts those facts as External Conflicting Context. To provide the mixed contexts, a supplementary context r_s and a conflicting context r_c are sampled from the dataset and interleaved with each other by every four tokens, and form a mixed context r_m .

Models Our evaluations are performed on five open-source LLMs, including Llama 2-7B, Llama 2-13B, Llama 2-70B (Touvron et al. 2023), Qwen3-8B (Team 2025), and DeepSeek-LLM-7B-base (DeepSeek-AI 2024).

Prompt of Multiple-Choice	
[INST] <<SYS>> According to the given information and your knowledge, choose the best choice from the following options. Follow the format: Option: your option. <</SYS>>	
• Question: <Query>	• Information: <External Context>
Options: A: <option a> B: <option b> [INST]	

Prompt of Open-ended QA	
[INST] <<SYS>> You are an assistant for question answering tasks. Use the following pieces of retrieved context and your own knowledge to answer the question. Among the multiple contexts retrieved, some are correct while others are incorrect. Use two sentences maximum and keep the answer concise. <</SYS>>	
• Question: <Query>	• Information: <External Context>
Answer:	[INST]

Figure 5: Prompt templates in conflicting scenarios.

Tasks and Metrics We include two primary tasks in our experiments to evaluate the response generation of Swin-VIB when LLM retrieves conflicting contexts, and the corresponding RAG performance:

1) *Multiple-choice*: This task can not only quantify the response generation preferences of LLMs but also can be used to evaluate the ability to exist methods to accommodate knowledge conflicts. Specifically, we provide two options for each query, one of which is obtained from the internal memory, and the other is from the external context. Only one option is correct, which constrains the generation space and yields confirmed answers.

- Memorization Preference Rate (MPR = $\frac{f_m}{S}$);
- Context Preference Rate (CPR = $\frac{f_c}{S}$);
- Uncertain Answer Rate (UAR = $\frac{S - f_m - f_c}{S}$);
- Accuracy Rate (ACC = $\frac{C_r}{S}$);
- Correction Rate (CR = $\frac{C_{crt}}{S - L}$);
- Resistance Rate (RR = $\frac{C_{def}}{L}$);
- Instance-level Uncertainty (Mean- ψ): Equal to the mean of the token-level negative log-likelihood values, its detailed computation procedure is provided in Appendix B.5;
- Total Response Entropy (TRE):
Equal to $-(ACC \log_2(ACC + \epsilon) + (1 - ACC - UAR) \log_2[(1 - ACC - UAR) + \epsilon] + UAR \log_2(UAR + \epsilon))$;

where S is the total number of dataset instances; f_m is the number of instances for which the LLM relies on internal memory, and f_c is the number of instances using external contexts. L is the number of instances for which the LLM can generate correct responses without any context. C_r is the number of instances for which the LLM can generate correct responses with conflicting contexts. C_{crt} counts instances that are answered incorrectly without external contexts but corrected after LLM retrieved external conflicting contexts. C_{def} counts instances that are answered correctly without external contexts and remain correctly answered after LLM retrieved conflicting contexts. ϵ is a small constant used to avoid numerical issues in logarithmic calculations.

2) *Open-ended QA*: We make the LLM generate responses, and evaluate response generation quality of RAG as well as

LLM	Method	ConflictQA						DRUID					
		ACC \uparrow	CR \uparrow	RR \uparrow	Mean- ψ \downarrow	UAR \downarrow	TRE \downarrow	ACC \uparrow	CR \uparrow	RR \uparrow	Mean- ψ \downarrow	UAR \downarrow	TRE \downarrow
Llama2-7B	Closed-book	20.61	-	-	0.31	-	-	50.58	-	-	0.34	-	-
	In-context	79.68	96.49	16.92	0.34	2.96	0.69	50.08	90.11	12.74	0.38	8.89	1.34
	CD ²	77.32	88.05	29.16	0.29	2.01	0.87	58.14	92.30	22.05	0.30	4.32	1.18
	Rowen-CL	80.10	92.59	28.55	0.28	1.30	0.79	52.35	94.76	17.30	0.29	5.92	1.26
	CK-PLUG	78.17	95.78	25.29	0.28	1.87	0.85	58.88	94.24	18.00	0.29	5.39	1.21
	Swin-VIB	84.04	98.18	29.40	0.24	0.21	0.64	63.24	94.87	25.63	0.26	2.85	1.09
Llama2-13B	Closed-book	21.37	-	-	0.30	-	-	50.93	-	-	0.33	-	-
	In-context	79.83	97.33	16.02	0.33	1.98	0.82	51.73	92.21	11.19	0.37	7.16	1.29
	CD ²	80.20	93.52	27.23	0.28	4.85	0.88	60.72	93.12	18.55	0.29	4.04	1.15
	Rowen-CL	80.36	95.42	28.55	0.27	1.10	0.76	52.61	94.85	16.93	0.28	4.36	1.21
	CK-PLUG	81.44	97.27	27.38	0.27	1.78	0.78	61.07	95.18	18.83	0.28	5.47	1.19
	Swin-VIB	85.68	99.59	30.40	0.23	0.18	0.61	63.43	95.16	25.48	0.25	1.96	1.06
Llama2-70B	Closed-book	20.99	-	-	0.29	-	-	49.59	-	-	0.32	-	-
	In-context	80.29	98.21	20.91	0.32	1.12	0.78	52.81	90.65	19.77	0.36	3.66	1.18
	CD ²	76.20	96.25	30.00	0.27	2.10	0.89	54.86	94.32	24.55	0.28	1.19	1.07
	Rowen-CL	81.43	97.04	29.46	0.26	0.95	0.74	54.44	95.60	23.89	0.26	0.97	1.06
	CK-PLUG	83.41	99.08	28.13	0.27	0.43	0.68	56.70	97.16	24.42	0.27	1.36	1.07
	Swin-VIB	87.68	99.48	31.06	0.22	0.03	0.54	62.94	96.86	27.37	0.24	0.16	0.97
DeepSeek-7B	Closed-book	16.42	-	-	0.30	-	-	37.93	-	-	0.33	-	-
	In-context	77.49	97.04	9.23	0.33	3.36	0.91	46.69	96.59	10.51	0.37	4.45	1.22
	CD ²	79.02	90.21	29.80	0.28	2.48	0.85	51.64	95.95	11.73	0.30	4.28	1.21
	Rowen-CL	81.83	96.29	50.20	0.28	2.32	0.78	43.49	94.21	9.87	0.28	4.77	1.22
	CK-PLUG	78.82	96.20	29.82	0.27	1.97	0.84	53.19	97.57	12.24	0.27	5.52	1.24
	Swin-VIB	84.13	98.83	58.65	0.24	0.79	0.68	56.39	98.75	16.55	0.27	1.97	1.10
Qwen3-8B	Closed-book	23.53	-	-	0.31	-	-	53.51	-	-	0.34	-	-
	In-context	78.36	97.25	15.89	0.34	2.11	0.85	56.88	96.12	12.24	0.38	3.44	1.16
	CD ²	74.42	95.18	26.44	0.30	3.06	0.96	57.60	98.58	12.49	0.32	3.97	1.17
	Rowen-CL	80.38	97.72	21.42	0.31	1.88	0.80	54.54	97.87	14.33	0.33	4.50	1.21
	CK-PLUG	78.61	96.11	28.15	0.29	1.89	0.84	57.86	98.52	16.78	0.29	3.50	1.17
	Swin-VIB	82.81	98.68	32.47	0.25	0.64	0.82	58.69	99.09	15.62	0.28	1.83	1.08

Table 2: Evaluation results of multiple-choice.

its robustness in real-world conflicting scenarios. For each query, to evaluate an open-ended QA with retrieved context, the top five correct or incorrect answers for a query are retrieved to fill the <external context> slot in the prompt template. The template is depicted in Figure 5. According to the experimental configuration of open-ended QA tasks (Yu, Zhang, and Feng 2024), we use EM and Faithfulness (Es et al. 2023) to evaluate whether the model can provide correct answers, as well as METEOR (Denkowski and Lavie 2014) to assess the quality of the response generation.

Baselines and Implementation Details We compare Swin-VIB with five SOTA baselines (Closed-book, In-context, CD² (Jin et al. 2024a), CK-PLUG (Bi et al. 2025), Rowen-CL (Ding et al. 2024)) on the multiple-choice task, while integrating Swin-VIB and these baselines into three advanced RAG methods (Naive RAG, Self-RAG (Asai et al. 2023), Astute RAG (Wang et al. 2024)) for the open-ended QA task (see their implementation details in Appendix B.4). We implement Swin-VIB with fixed-length sliding windows (7 tokens) and set (ξ, β) to $(0.68, 10^{-5})$ on all datasets. Data preprocessing, hardware/software environment, and model configurations are described in Appendix B.1–B.3. During the training stage, the bottleneck loss converges within ≈ 200 epochs, and deeper decoder layers provide more robustness (see Appendix C.2 for convergence analysis). Swin-VIB achieves advanced generation quality to β in the range 10^{-5} – 10^{-3} , and remains stable when the threshold ξ lies between 0.60 and 0.8. A window length of 7 tokens can trade off accuracy and inference latency. The windows with fewer tokens degrade the precision to accept these windows, whereas the windows with more than 7 tokens also slightly degrade ac-

ceptance precision. The parameters β and ξ , and the window length are analyzed in Appendix C.3.

4.2 Verification of Our Theoretical Analysis

To verify our theoretical analysis 2.2, we explore the impact of information difference on LLMs’ preference and generation uncertainty on the multiple-choice task. To achieve that, the internal-memory facts (supplementary information) are collected and combined into the external context with controlled proportions. As depicted in Figure 2, we get two observations:

- The preferences of the LLM are influenced by the proportion of external conflicting and supplementary information. As the information difference grows, LLM becomes more focused on a certain preference, and the curve in Figure 2 mirrors this trajectory. (see Appendix C.1 for analysis of answer preference distributions)
- When the proportions are set at 2:2, the UAR values reach their maximum. This indicates that when the information difference is slight, the uncertainty of response generation is the greatest. The empirical “rise–then–fall” trend of the UAR in Figure 6 is consistent with the curve in Figure 2.

4.3 Comparisons with State of the Arts

Through the comparison of Swin-VIB and baselines, we can observe the following in Table 2: Swin-VIB significantly outperforms the state-of-the-art baselines on all settings and outperforms the strongest baseline by up to 6.24%. This demonstrates its robustness of response generation in the conflicting scenario. Swin-VIB attains the best trade-off between CR and RR, reflecting both strong capability for error

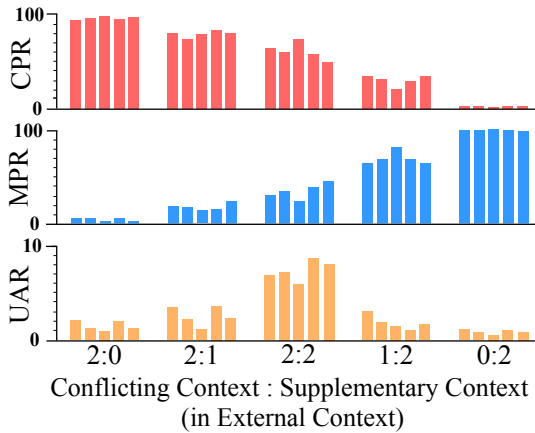


Figure 6: The uncertainty answer ratio of LLMs under varying proportions of external conflicting information from ConflictQA, e.g., 1:2, means that the external context includes one conflicting context and two supplementary contexts. For each bar group, the results for different LLMs are listed according to the order of Llama2-7B, Llama2-13B, Llama2-70B, Deepseek-7B and Qwen3-8B.

recovery and resilience to misleading context. This enables Swin-VIB to generate more reliable responses. On the other hand, it considerably reduces UAR, so the LLMs have less probability of skipping answering the queries. To specifically measure the uncertainty of response generation, following the literature (Zhu et al. 2024), we take the output distribution of the LLM to measure the macro-level uncertainty of LLMs with the metric, total response entropy (TRE). The corresponding results prove that the adaptation principle of Swin-VIB is quite effective in accommodating knowledge conflicts and improving response reliability. Similarly, the decrease in Mean- ψ confirms that Swin-VIB maintains smaller micro-level uncertainty. Actually, the Pearson correlation between $Mean - \psi$ and TRE is 0.81 (see Appendix C.5), validating the high robustness of Swin-VIB. Finally, to verify whether Swin-VIB has selected the windows with larger information difference, we conducted a small-scale human annotation study. We find that 76 % of the windows discarded by Swin-VIB were judged “undecidable” (no clear conflicting or supplementary information) and the result confirms that our method indeed amplifies the information difference in a rational way (see Appendix C.6).

4.4 Evaluation of RAG with Swin-VIB

This section examines how integrating Swin-VIB into advanced RAG frameworks, enhances practical applicability under real-world settings, including evaluating generation quality and inference latency.

As shown in Table 3, Astute-RAG employs an iterative fusion step in a data augmented stage, and thus raises decision variance and generation uncertainty. From the beginning, Swin-VIB drops the windows with high uncertainty context, alleviates Astute-RAG’s uncertainty, and achieves an improvement of EM by 11.14%. Additionally, we observe a

Methods	EM \uparrow	Meteor \uparrow	Faithfulness \downarrow
Naive RAG	46.50	42.85	73.03
Naive RAG + Swin-VIB	60.14	50.95	66.58
Self-RAG	39.39	43.38	70.10
Self-RAG + Swin-VIB	58.32	55.29	64.32
Astute RAG	53.02	44.69	65.23
Astute RAG + Swin-VIB	64.16	53.70	64.09

Table 3: Evaluation of Open-ended QA tasks on TruthfulQA

significant reduction in faithfulness by 6.45%, indicating that the LLM no longer copies the retrieved context totally. This is because the sliding-window strategy of Swin-VIB trades some cross-segment coherence for higher intra-segment consistency. On the other hand, the naive RAG and Self-RAG lack conflicting accommodation resolution, often copy the retrieved context, and fall behind on both EM and METEOR. The high EM scores of Swin-VIB show that it can adapt the LLM’s preference on external contexts and select the most relevant external information, even when the top-5 retrieved contexts contain conflicting information. These results demonstrate that Swin-VIB can improve response generation quality and reliability for mitigating knowledge conflicts in RAG.

LLM	Naive RAG	Our cost per window \downarrow	Our cost \downarrow
Llama2-7B	0.4912s	0.08ms	0.3913s
Llama2-13B	0.8791s	0.14ms	0.5221s
Llama2-70B	4.6013s	0.55ms	2.7830s
Qwen3-8B	0.3862s	0.12ms	0.2740s
DeepSeek-7B	0.3770s	0.11ms	0.4293s

Table 4: Efficiency Evaluation of Open-ended QA tasks on TruthfulQA

Table 4 evaluates the overhead of Swin-VIB in response generation delay. For Llama2-7B, Swin-VIB involves an additional delay of 0.3913 seconds. It can also be found that after the Swin-VIB has been integrated into the RAG systems, the increased number of model parameters does not significantly increase the latency. The Rag systems remain sufficiently lightweight, since Swin-VIB trades off efficiency and accuracy in response generation. (see Appendix C.4 for computational complexity analysis).

5 Related Work

Efforts to mitigate risks associated with knowledge conflicts in response generation can be categorized into three groups: a) Internal knowledge-driven methods (Shi et al. 2023b; Jin et al. 2024b; Zhang, Yu, and Feng 2024): Fine-tuning or editing the model so that the retrieved evidences can override conflicts; b) External-validation methods incorporate verification module to ensure the reliability of retrieved contexts (Yu, Zhang, and Feng 2024; Kortukov et al. 2024; Bi et al. 2025); c) Adaptive methods at the decoding stage, take LLM parameters frozen and detect token-level conflicts through adjusting parametric and context logits (Shi et al. 2023a; Yuan et al. 2024; Jin et al. 2024a; Bi et al. 2025; Huang et al. 2025). However, these existing methods have limitations in

elucidating LLMs' knowledge preference due to: a) Internal catastrophic forgetting of LLMs caused by fine-tuning (Xu et al. 2024), b) Overconfidence in external sources caused by external validation (Xie et al. 2023); c) Adaptive single-token adjustments struggling with long text analysis, thus limiting their practical applicability in real-world RAG deployments. The recent empirical works (Jin et al. 2024b; Zhao et al. 2024; Yuan et al. 2025) focus on heuristic interventions on response generation of LLMs.

In contrast, our theoretical study demonstrates that the information difference between external context and internal representations is the true force to drive preference shifts and information selection. According to this insight, we propose a novel response generation method (Li et al. 2024), Swin-VIB. Its bottleneck-based adapter is involved to regulate the compression ratio of the retrieved information, without retraining the pre-trained LLMs. In this way, Swin-VIB accommodates conflicting knowledge, avoiding merely relying on internal or external information. This information-theoretic insight furnishes a unified, model-agnostic yardstick that combines theoretical breadth with practical simplicity.

6 Conclusion

This work proposes a novel theoretical framework to analyze and address the issue of information conflicts encountered by LLMs in RAG systems. Leveraging analysis on the knowledge conflicts and preferences of LLMs from an information theory perspective, we find that the uncertainty of LLMs can be mitigated by adapting the external information difference of LLMs. Insight from this, we propose Swin-VIB to optimize how RAG handles external contexts to achieve reliable response generation. Experimental results demonstrate that Swin-VIB significantly accommodates conflicts, reduces uncertainty in LLM outputs, and generates more accurate, consistent, and context-aware responses. Moreover, Swin-VIB enhances retrieval system performance, facilitating its real-world applications. Future work will explore extending this approach to more types of response generation tasks to validate further and to improve its effectiveness.

Acknowledgments

This work is partially supported by the National Natural Science Foundation of China (62272248 and 61962045), the Natural Science Foundation of Tianjin (25JJJC0016, 23JCZDJC01010 and 25JCZDSN00040), in part by the Program for Young Talents of Science and Technology in Universities of Inner Mongolia Autonomous Region under Grant NJYT23104, and the Basic Scientific Research Expenses Program of Universities directly under Inner Mongolia Autonomous Region under Grant JY20220273 and Grant JY20240002.

References

Alemi, A. A.; Fischer, I.; Dillon, J. V.; and Murphy, K. 2016. Deep variational information bottleneck. *arXiv preprint arXiv:1612.00410*.

Asai, A.; Wu, Z.; Wang, Y.; Sil, A.; and Hajishirzi, H. 2023. Self-rag: Learning to retrieve, generate, and critique through self-reflection. *arXiv preprint arXiv:2310.11511*.

Bi, B.; Liu, S.; Wang, Y.; Xu, Y.; Fang, J.; Mei, L.; and Cheng, X. 2025. Parameters vs. Context: Fine-Grained Control of Knowledge Reliance in Language Models. *arXiv preprint arXiv:2503.15888*.

Brown, T.; Mann, B.; Ryder, N.; Subbiah, M.; Kaplan, J. D.; Dhariwal, P.; Neelakantan, A.; Shyam, P.; Sastry, G.; Askell, A.; et al. 2020. Language models are few-shot learners. *Advances in neural information processing systems*, 33: 1877–1901.

DeepSeek-AI. 2024. DeepSeek LLM: Scaling Open-Source Language Models with Longtermism. *arXiv preprint arXiv:2401.02954*.

Denkowski, M.; and Lavie, A. 2014. Meteor universal: Language specific translation evaluation for any target language. In *Proceedings of the ninth workshop on statistical machine translation*, 376–380.

Ding, H.; Pang, L.; Wei, Z.; Shen, H.; and Cheng, X. 2024. Retrieve only when it needs: Adaptive retrieval augmentation for hallucination mitigation in large language models. *arXiv preprint arXiv:2402.10612*.

Elastic. 2023. Elasticsearch. <https://www.elastic.co/guide/en/elasticsearch/reference/current/elasticsearch-intro-what-is-es.html>. Accessed: 2023-10-10.

Es, S.; James, J.; Espinosa-Anke, L.; and Schockaert, S. 2023. Ragas: Automated evaluation of retrieval augmented generation. *arXiv preprint arXiv:2309.15217*.

Gao, Y.; Xiong, Y.; Gao, X.; Jia, K.; Pan, J.; Bi, Y.; Dai, Y.; Sun, J.; Wang, H.; and Wang, H. 2023. Retrieval-augmented generation for large language models: A survey. *arXiv preprint arXiv:2312.10997*, 2: 1.

Hagström, L.; Marjanović, S. V.; Yu, H.; Arora, A.; Lioma, C.; Maistro, M.; Atanasova, P.; and Augenstein, I. 2024. A Reality Check on Context Utilisation for Retrieval-Augmented Generation. *arXiv preprint arXiv:2412.17031*.

Huang, P.; Liu, Z.; Yan, Y.; Yi, X.; Chen, H.; Liu, Z.; Sun, M.; Xiao, T.; Yu, G.; and Xiong, C. 2025. Pip-kag: Mitigating knowledge conflicts in knowledge-augmented generation via parametric pruning. *arXiv preprint arXiv:2502.15543*.

Jin, Z.; Cao, P.; Chen, Y.; Liu, K.; Jiang, X.; Xu, J.; Li, Q.; and Zhao, J. 2024a. Tug-of-war between knowledge: Exploring and resolving knowledge conflicts in retrieval-augmented language models. *arXiv preprint arXiv:2402.14409*.

Jin, Z.; Cao, P.; Yuan, H.; Chen, Y.; Xu, J.; Li, H.; Jiang, X.; Liu, K.; and Zhao, J. 2024b. Cutting Off the Head Ends the Conflict: A Mechanism for Interpreting and Mitigating Knowledge Conflicts in Language Models. *arXiv preprint arXiv:2402.18154*.

Kingma, D. P.; and Welling, M. 2013. Auto-encoding variational bayes. *arXiv preprint arXiv:1312.6114*.

Kong, I.; and Kim, Y. 2024. Posterior concentrations of fully-connected Bayesian neural networks with general priors on the weights. *arXiv preprint arXiv:2403.14225*.

- Kortukov, E.; Rubinstein, A.; Nguyen, E.; and Oh, S. J. 2024. Studying large language model behaviors under realistic knowledge conflicts. *arXiv e-prints*, arXiv-2404.
- Lewis, P.; Perez, E.; Piktus, A.; Petroni, F.; Karpukhin, V.; Goyal, N.; Küttler, H.; Lewis, M.; Yih, W.-t.; Rocktäschel, T.; et al. 2020. Retrieval-augmented generation for knowledge-intensive nlp tasks. *Advances in Neural Information Processing Systems*, 33: 9459–9474.
- Li, X.; Jin, J.; Zhou, Y.; Zhang, Y.; Zhang, P.; Zhu, Y.; and Dou, Z. 2024. From matching to generation: A survey on generative information retrieval. *arXiv preprint arXiv:2404.14851*.
- Lin, S.; Hilton, J.; and Evans, O. 2021. Truthfulqa: Measuring how models mimic human falsehoods. *arXiv preprint arXiv:2109.07958*.
- OpenAI. 2023. GPT-4 Technical Report. *arXiv preprint arXiv:2303.08774*.
- Polson, N. G.; and Ročková, V. 2018. Posterior concentration for sparse deep learning. *Advances in neural information processing systems*, 31.
- Robertson, S. E.; and Jones, K. S. 1976. Relevance weighting of search terms. *Journal of the American Society for Information science*, 27(3): 129–146.
- Shannon, C. E. 1948. A mathematical theory of communication. *The Bell system technical journal*, 27(3): 379–423.
- Shi, W.; Han, X.; Lewis, M.; Tsvetkov, Y.; Zettlemoyer, L.; and Yih, S. W.-t. 2023a. Trusting your evidence: Hallucinate less with context-aware decoding. *arXiv preprint arXiv:2305.14739*.
- Shi, W.; Min, S.; Lomeli, M.; Zhou, C.; Li, M.; Lin, V.; Smith, N. A.; Zettlemoyer, L.; Yih, S.; and Lewis, M. 2023b. In-context pretraining: Language modeling beyond document boundaries. *arXiv preprint arXiv:2310.10638*.
- Team, Q. 2025. Qwen3 Technical Report. arXiv:2505.09388.
- Tishby, N.; Pereira, F. C.; and Bialek, W. 2000. The information bottleneck method. *arXiv preprint physics/0004057*.
- Touvron, H.; Martin, L.; Stone, K.; Albert, P.; Almahairi, A.; Babaei, Y.; Bashlykov, N.; Batra, S.; Bhargava, P.; Bhosale, S.; et al. 2023. Llama 2: Open foundation and fine-tuned chat models. *arXiv preprint arXiv:2307.09288*.
- Wang, F.; Wan, X.; Sun, R.; Chen, J.; and Arik, S. Ö. 2024. Astute rag: Overcoming imperfect retrieval augmentation and knowledge conflicts for large language models. *arXiv preprint arXiv:2410.07176*.
- Wang, Y.; Sun, Q.; and He, S. 2023. M3E: Moka Massive Mixed Embedding Model. Online. Accessed: 2025-11-15.
- Wu, K.; Wu, E.; and Zou, J. 2024. How faithful are RAG models? Quantifying the tug-of-war between RAG and LLMs’ internal prior. *arXiv preprint arXiv:2404.10198*.
- Xie, J.; Zhang, K.; Chen, J.; Lou, R.; and Su, Y. 2023. Adaptive chameleon or stubborn sloth: Revealing the behavior of large language models in knowledge conflicts. In *The Twelfth International Conference on Learning Representations*.
- Xu, R.; Qi, Z.; Wang, C.; Wang, H.; Zhang, Y.; and Xu, W. 2024. Knowledge Conflicts for LLMs: A Survey. *arXiv preprint arXiv:2403.08319*.
- Yu, T.; Zhang, S.; and Feng, Y. 2024. Truth-aware context selection: Mitigating hallucinations of large language models being misled by untruthful contexts. *arXiv preprint arXiv:2403.07556*.
- Yuan, X.; Yang, Z.; Huang, Z.; Wang, Y.; Fan, S.; Ju, Y.; Zhao, J.; and Liu, K. 2025. Exploiting Contextual Knowledge in LLMs through V-usable Information based Layer Enhancement. *arXiv preprint arXiv:2504.15630*.
- Yuan, X.; Yang, Z.; Wang, Y.; Liu, S.; Zhao, J.; and Liu, K. 2024. Discerning and resolving knowledge conflicts through adaptive decoding with contextual information-entropy constraint. *arXiv preprint arXiv:2402.11893*.
- Zhang, S.; Yu, T.; and Feng, Y. 2024. Truthx: Alleviating hallucinations by editing large language models in truthful space. *arXiv preprint arXiv:2402.17811*.
- Zhao, Y.; Devoto, A.; Hong, G.; Du, X.; Gema, A. P.; Wang, H.; He, X.; Wong, K.-F.; and Minervini, P. 2024. Steering knowledge selection behaviours in LLMs via sae-based representation engineering. *arXiv preprint arXiv:2410.15999*.
- Zhu, T.; Liu, Q.; Wang, F.; Tu, Z.; and Chen, M. 2024. Unraveling cross-modality knowledge conflicts in large vision-language models. *arXiv preprint arXiv:2410.03659*.

Technical Appendix for Accommodate Knowledge Conflicts in Retrieval-augmented LLMs: Towards Robust Response Generation in the Wild

A Theoretical Analysis

A.1 Factorising Conditional Entropy

Without a theoretical analysis of knowledge conflicts, the limitations of empirical rules and experimental settings in response generation can hardly be alleviated (Xu et al. 2024; Wu, Wu, and Zou 2024; Xie et al. 2023; Jin et al. 2024a). To tackle this challenge, we propose a theoretical framework that shows knowledge conflicts can be defined by conditional entropy, the corresponding symbol system is defined in Table 5. Based on Definition 1 (Uncertainty, main paper), we derive

Table 5: Symbols and their meanings

Symbol	Meaning
Q	Queries
$R = B(Q)$	External contexts from the knowledge base B
$O = LLM(R, Q)$	Generated Responses by LLM

from the law of total probability and the chain rule:

$$\begin{aligned} \mathbb{H}(O | R, Q) &= - \sum_{q,r,o} p(q) p(r | q) p(o | r, q) \log p(o | r, q) \\ &= \sum_q p(q) \sum_r p(r | q) \sum_o \psi(p(o | r, q)). \end{aligned} \quad (15)$$

Let $\psi(\cdot)$ denote instance-level uncertainty, and be calculated by

$$\psi(p(o | r, q)) = -p(o | r, q) \log p(o | r, q) \quad (16)$$

A.2 Decomposing Conflicting and Supplementary Information

$p(o | r, q)$ can be derived as the follows:

$$\begin{aligned} p(o | r, q) &= \int_X p(o | r, q, x) p(x | r, q) dx, \\ &\quad // \text{marginalization} \\ &= \int_X p(o | r, q, x) \frac{p(r, q | x) p(x)}{p(r, q)} dx, \\ &\quad // \text{Bayes' Theorem} \\ &\propto \int_X p(o | r, q, x) p(r, q | x) p(x) dx, \\ &\quad // p(r, q) \text{ is a constant} \\ &\propto \int_X p(o | r, q, x) \frac{p(r, q | x)}{p(r, q | x_\gamma)} p(x) dx, \\ &\quad // p(r, q | x_\gamma) \text{ is a constant} \\ &= \int_X p(o | r, q, x) \exp \left[\log \frac{p(r, q | x)}{p(r, q | x_\gamma)} \right] p(x) dx \\ &= \int_X p(o | r, q, x) \exp \left[\underbrace{\log \frac{p(q | r, x)}{p(q | r, x_\gamma)}}_{\delta_q(r, x)} + \log \frac{p(r | x)}{p(r | x_\gamma)} \right] p(x) dx. \\ &\approx \int_X p(o | r, q, x) \exp \left[\log \mathcal{B} + \log \frac{p(r | x)}{p(r | x_\gamma)} \right] p(x) dx \\ &\approx \int_X p(o | r, q, x) \exp \left[\log p(r | x) - \log p(r | x_\gamma) \right] p(x) dx \end{aligned} \quad (17)$$

where X denotes the high-dimensional latent space of the LLM containing all embedded information that may affect response generation; x is a recalled instance sampled from X . Let $\delta_q(r, x) = \log \frac{p(q | r, x)}{p(q | r, x_\gamma)}$, and $s(x) = \log p(r, q | x)$

be the retriever score and x_γ is a top-ranked latent state that coincides with information retrieved from an external text or database, while considering query q . So $s(x_\gamma) \geq s(x)$ and

$$\log \frac{p(r, q | x_\gamma)}{p(r, q | x)} \geq 0. \quad (18)$$

Using Bayes' rule, this fraction can be divided:

$$\begin{aligned} \delta_q(r, x) &= \log \frac{p(r, q | x)}{p(r, q | x_\gamma)} + \log \frac{p(r | x_\gamma)}{p(r | x)} \\ &\leq \log \frac{p(r | x_\gamma)}{p(r | x)} = \log \mathcal{B}(r, x), \end{aligned} \quad (19)$$

which keeps $e^{\delta_q(r, x)}$ uniformly bounded on the candidate set. Around x_γ , a first-order expansion gives

$$e^{\delta_q(r, x)} = e^{\delta_q(r, x_\gamma)} [1 + \mathcal{O}(\|x - x_\gamma\|)]. \quad (20)$$

The factor $e^{\delta_q(r, x_\gamma)}$ is independent of o , and the residual $\mathcal{O}(\|x - x_\gamma\|)$ is small to the integral. Therefore, in

$$\begin{aligned} p(o | r, q) &= \int_X p(o | r, q, x) e^{\delta_q(r, x_\gamma)} [1 + \mathcal{O}(\|x - x_\gamma\|)] \\ &\quad \exp\left[\log \frac{p(r|x)}{p(r|x_\gamma)}\right] dx, \end{aligned} \quad (21)$$

Any factor that does not depend on o can be absorbed by normalization (equivalently, by normalizing the weights over x). Therefore we use

$$p(o | r, q) \propto \int_X p(o | r, q, x) \exp\left[\log \frac{p(r|x)}{p(r|x_\gamma)}\right] p(x) dx. \quad (22)$$

and drop δ_q thereafter since it only induces a first-order (small) perturbation of the weights.

A.3 First-Order Approximation

The self-information of $-\log p(\cdot)$ quantifies how much information is revealed (Shannon 1948). We categorize the external information retrieved from an external text or database into two types, whereas the LLMs' pre-trained knowledge is either contradicted or insufficient.

- *Conflicting Information:* If the retrieved information instance contradicts x_γ in the LLMs' pre-trained knowledge, quantified by $I_c = -\log p(r | x_\gamma)$.
- *Supplementary Information:* If the retrieved information is complementary to the external context and quantified $I_s = -\log p(r | x)$.

According to Formula 22, we write

$$p(o | r, q) \propto \int_X p(o | r, q, x) \exp[I_c - I_s] p(x) dx. \quad (23)$$

From Eq. (23) we have

$$p(o | r, q) \propto e^{I_c} \int_X p(o | r, q, x) e^{-I_s(x)} p(x) dx, \quad (\text{A.8})$$

Let $w(x) = p(o | r, q, x) e^{-I_s(x)} p(x)$, $\phi(x) = -\log w(x)$. Because $p(x | r, q)$ for LLMs is sharply peaked (Polson

and Ročková 2018; Kong and Kim 2024), $w(x)$ is concentrated in a narrow region around a local minimum $x^* = \arg \min_x \phi(x)$ (equivalently, a maximum of w). A second-order Taylor expansion of ϕ around x^* yields

$$\phi(x) \approx \phi(x^*) + \frac{1}{2}(x - x^*)^\top H(x^*)(x - x^*), \quad (24)$$

where H is the Hessian. Evaluating the Gaussian integral gives

$$p(o | r, q) \approx \tilde{C}(o) \exp[I_c - I_s(x^*)] + \mathcal{O}(\varepsilon^2), \quad (\text{A.9})$$

where $\tilde{C}(o)$ collects terms independent of x (and ε characterises the local width). After normalising over o , constants such as $\tilde{C}(o)$ cancel, so the relative probability is proportional to $\exp[I_c - I_s(x^*)]$. Since \exp is strictly increasing,

$$\Delta I = I_c - I_s(x^*). \quad (25)$$

We use the first-order linear proxy

$$\exp(\Delta I) \approx 1 + \Delta I, \quad (26)$$

hence $p(o | r, q) \propto \Delta I$. Larger $|\Delta I|$ pushes the LLM towards the source (conflicting information vs. supplementary information) that better explains the retrieved context, thereby increasing the relative weight of answers consistent with that source.

To connect the above approximation with uncertainty in a minimal form, let $a_o := \tilde{C}(o) > 0$ and $b_o := \Delta I(o) = I_c - I_s(x^*(o))$, and for $\alpha > 0$ define $p_\alpha(o) = \frac{a_o e^{\alpha b_o}}{Z(\alpha)}$ with $Z(\alpha) = \sum_o a_o e^{\alpha b_o}$ and $\Psi_\alpha(r, q) = -\sum_o p_\alpha(o) \log p_\alpha(o)$. Differentiating (using $\frac{d}{d\alpha} \log Z = \mathbb{E}_{p_\alpha}[b]$ and $\frac{d}{d\alpha} \mathbb{E}_{p_\alpha}[f] = \text{Cov}_{p_\alpha}(f, b)$) gives

$$\frac{d}{d\alpha} \Psi_\alpha(r, q) = -\alpha \text{Var}_{p_\alpha}(b) - \text{Cov}_{p_\alpha}(\log a_o, b) \leq 0, \quad (27)$$

with strict inequality unless b_o is constant. Since a_o varies slowly, the variance term dominates, so increasing the contrast $|\Delta I|$ makes p_α more peaked and lowers $\Psi_\alpha(r, q)$. Averaging over $p(q)p(r | q)$ implies $\mathbb{H}(O | R, Q)$ decreases in expectation. (Monotonicity relies on the derivative above; the linear proxy $\exp(\Delta I) \approx 1 + \Delta I$ is only for intuition.)

A.4 Uncertainty Drop and Information

Without retrieval, the LLM outputs a baseline distribution p_0 . After adding a retrieved context r , the output becomes p . Let $p_0(o) = p(o | q)$ and denote $p(o | r, q)$ by $p(o)$. Define

$$Z(o) = \log p(o) - \log p_0(o), \quad o \sim p_0. \quad (28)$$

By Jensen's inequality,

$$\mathbb{E}_{p_0}[Z] \leq 0 \quad \Rightarrow \quad U := -\mathbb{E}_{p_0}[Z] = \text{KL}(p_0 \| p) \geq 0, \quad (29)$$

where U is a computable proxy that measures how far the augmented output p moves from the baseline p_0 . According to instance-level uncertainty $\psi(u) = -u \log u$ for $u \in [0, 1]$, and the entropy of a distribution as $\Psi(p) = \sum_o \psi(p(o))$. The entropy change is

$$\Delta \Psi = \Psi(p) - \Psi(p_0) = \sum_o [p_0(o) \log p_0(o) - p(o) \log p(o)], \quad (30)$$

which indicates whether augmentation makes the model more confident ($\Delta\Psi < 0$). Consistent with Sec. 2 of the main manuscript, when the information difference $|\Delta I|$ between conflicting and supplementary information is larger, the deviation $U = \text{KL}(p_0||p)$ tends to increase and we typically observe an entropy drop ($\Delta\Psi < 0$). Thus, a marked decrease in entropy serves as a practical indicator that the information difference has increased, even though U (an output-space proxy) is not the same as the latent-space quantity $|\Delta I|$.

B Implement Details

B.1 Dataset Processing Details

ConflictQA ConflictQA (Xie et al. 2023) is a benchmark for studying knowledge conflicts. This dataset provides LLM’s internal memory and information supporting the external context for each query. To explore the information differences from different ratios in empirical verification of LLM’s preference, it provides two supplementary contexts supporting the LLM’s internal memory ("parametric memory", "parametric memory aligned evidence") and two conflicting contexts supporting the counter answer ("counter memory", "counter memory aligned evidence") for every query.

DRUID DRUID (Hagström et al. 2024) contains real-world (query, context) pairs to facilitate studies of context usage and failures. For a multiple-choice task using the DRUID dataset, for each unique "claimant", we select two mutually exclusive "claims" from the dataset as the answer options. Each selected "claim" must have at least one evidence entry marked as either supports or insufficient-supports. The corresponding evidence entries serve as the context for each answer option. The evidence associated with the verified claim is treated as the supplementary context, whereas the evidence for the refuted claim is treated as the conflicting context. If a "claimant" lacks two conflicting claims, we skip that "claimant" and proceed to the next. The ground truth for each question is determined by the "factcheck-verdict": the "claim" with "factcheck-verdict=True" is considered correct. If both claims have "factcheck-verdict=False", we randomly select one "claim" as the ground truth to maintain consistency in the evaluation.

TruthfulQA TruthfulQA (Lin, Hilton, and Evans 2021) evaluates LLM truthfulness across 817 questions, each paired with one best, several correct, and several incorrect answers. Specifically, to implement seamless integration, an Elasticsearch-based retrieval system (Elastic 2023) with an embedding model named m3e-base (Wang, Sun, and He 2023) and a database named TruthfulQA is constructed. For each query, we retrieve the top five correct or incorrect responses to fill the slot `<external context>` in the corresponding templates (see Figure 7). Among these retrieved candidates, the one selected by our LLM is the supplementary context, while unselected candidates collectively form the conflicting context. Finally, we use the "best answer" key in TruthfulQA as the ground truth for evaluating Swin-VIB’s performance in RAG.

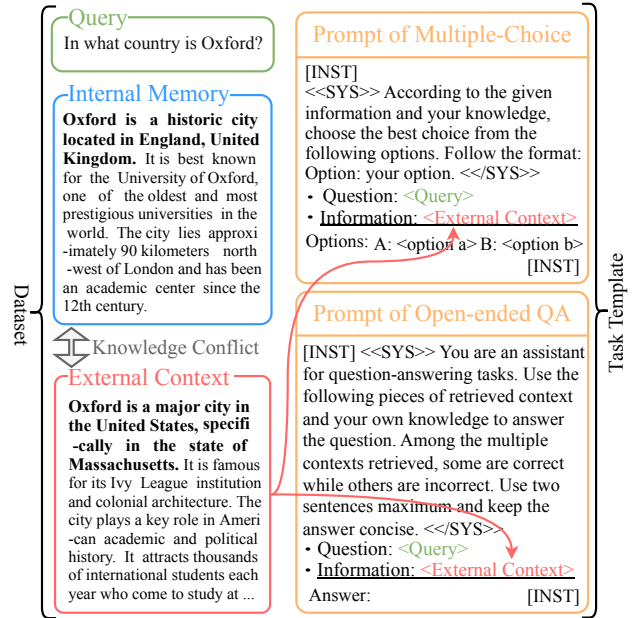


Figure 7: Our framework for simulating knowledge conflicts.

Mixed Context To provide the mixed contexts, a supplementary context and a conflicting context are sampled from the dataset and interleave with each other by every four tokens, forming a mixed context.

Table 6: Dataset information

Dataset	Size	Task	
		Multiple-choice	Open-ended QA
ConflictQA	2839	✓	
DRUID	1003	✓	
TruthfulQA	817		✓

Simulated Conflict Generation For LLMs not included in the dataset, we uniformly construct conflict scenarios in the following manner: First, each query from the dataset is posed to the LLM in a closed-book setting, so the LLM’s response and accompanying rationale are treated as its bona fide internal memory; Second, we prompt ChatGPT (OpenAI 2023) to draft a coherent passage whose factual content contradicts that of its internal memory. The overall procedure is illustrated in Figure 7.

B.2 Hardware and Software Environment

Experiments were run on Ubuntu 20.04 with NVIDIA RTX A6000 GPUs under PyTorch 2.4.1.

B.3 Model Configuration

A variational information-bottleneck network that first maps the 3584-dimensional input through a linear layer to 2048 units, followed by batch normalization, ReLU activation, and 50% dropout. The encoder splits into two parallel linear heads ($2,048 \rightarrow 512$), producing the latent mean μ and log-variance $\log \sigma^2$. Using the reparameterization trick, the latent vector

\mathbf{Z} is sampled and fed into a three-stage decoder: $512 \rightarrow 256$ (with batch normalization, ReLU, and dropout), $256 \rightarrow 128$ (with batch normalization, ReLU, and dropout), and finally $128 \rightarrow 1$. A sigmoid transforms the final logit into a probability. Training minimizes binary-cross-entropy for prediction accuracy plus a KL-divergence term that regularizes μ and σ^2 , weighted by the β hyperparameter. The reported results are based on a two-fold cross-validation.

B.4 Implementation details for each baseline

We compare Swin-VIB with five baselines on the multiple-choice and plug it into three advanced RAG methods for open-ended QA:

- Closed-book: LLM answers without any external context
- In-context: Conflicting context is added to the prompt
- CD² (Jin et al. 2024a): Each option undergoes two forward passes, computing log-probabilities on the bare question and with conflicting context; the option with the larger weighted difference is chosen..
- CK-PLUG (Bi et al. 2025): Evaluation procedures identical to CD².
- Rowen-CL (Ding et al. 2024): invokes the Serper Google Search API to retrieve auxiliary Information whenever its consistency score drops below 0.6.
- Naive RAG: Based on TruthfulQA, an Elasticsearch-based retriever (Elastic 2023) indexed with m3e-base embeddings (Wang, Sun, and He 2023) (index name TruthfulQA) is built.
- Self-RAG (Asai et al. 2023): Adaptive retrieval threshold = 0.2, ndocs = 5.
- Astute RAG (Wang et al. 2024): Final answer chosen by reliability-weighted voting (default $\tau = 0.7$).

For all methods, we use the recommended config for fair comparisons.

B.5 Instance-level uncertainty

Given a query q and a retrieved context r , let the language model generate an answer $o = (o_1, \dots, o_{|o|})$ of length $|o|$ tokens. We define the instance-level uncertainty of this generation as the average token-wise negative log-likelihood:

$$\psi(q, r) = -\frac{1}{|o|} \sum_{t=1}^{|o|} \log P(o_t | o_{<t}, q, r), \quad (31)$$

where $o_{<t} = (o_1, \dots, o_{t-1})$ denotes the prefix generated before step t . A more confident LLM places higher probability mass on the realised answer tokens o_t , leading to a lower value of $\psi(q, r)$. For a dataset containing S samples $\{(q_i, r_i)\}_{i=1}^S$, we report the mean uncertainty

$$\text{Mean-}\psi = \frac{1}{S} \sum_{i=1}^S \psi(q_i, r_i), \quad (32)$$

which summarises the model’s overall confidence across the corpus.

C Supplementary Experiments

C.1 Answer-Preference Distribution Across Models and Datasets

Knowledge conflicts may cause uncertainty in RG because LLMs must choose between internal memory and external context. In this paper, we conduct controlled experiments to construct knowledge conflicts. We evaluated five LLMs on the multiple-choice task, as shown in Figure 8. Llama-2-7B and Llama-2-70B differ by 22.77% in CPR and by 28% in MPR on DRUID. These results reveal substantial cognitive divergence among the dataset’s model-specific knowledge representations. Even the same LLM has obvious differences in preferences on different input distributions. For example, Llama-2-70B has different preferences on two datasets, which may be due to the bias of the training corpus. So our controlled experiments reveal that this answer-preference is highly idiosyncratic: it varies not only across models but also across datasets. Consistent with this observation, we deliberately extract attention representations that are specific to each model–dataset pair rather than using a single, global representation. Aligning the representation granularity with the observed preference patterns ensures that our method faithfully captures the factors driving each model’s decisions and avoids spurious, cross-dataset generalization.

C.2 Training Convergence Analysis

In this section, we evaluated convergence analysis and layer-wise prediction performance based on the multiple-choice task.

Convergence Analysis Figure 9(a) depicts the convergence of the bottleneck module trained on Qwen3-8B’s first block on the ConflictQA: the information-bottleneck loss \mathcal{L} plateaus after ≈ 200 epochs, evidencing rapid optimization and confirming the loss term’s effectiveness.

Layer-wise Prediction Performance For each decoder block, we project the last-token hidden state through the tied LM head to obtain logits, then apply softmax, and compare the resulting log-likelihoods of the answer tokens (e.g., “A” vs. “B”). The higher-scoring token yields a depth-indexed multiple-choice prediction. At the same time, we evaluate the bottleneck training on a validation dataset. As shown in Figure 9(b), we observe that the layer-wise information-bottleneck heads consistently outperform the vanilla LLM outputs. The gains occur because the bottleneck isolates high-dimensional discrepancy features that are strongly correlated with epistemic uncertainty. In addition, deeper layers of the LLM handle knowledge conflicts more accurately and with lower variance; however, a few layers (e.g., layers 10 and 17) display pronounced outlier behavior. We advocate weight-averaging the layer-level predictions when forming the final answer to mitigate the latter’s adverse influence at test time.

C.3 Ablation and Sensitivity Studies

In this section, we evaluated β -Scaling, sliding-window length study, and Sensitivity to the threshold ξ based on the multiple-choice task.

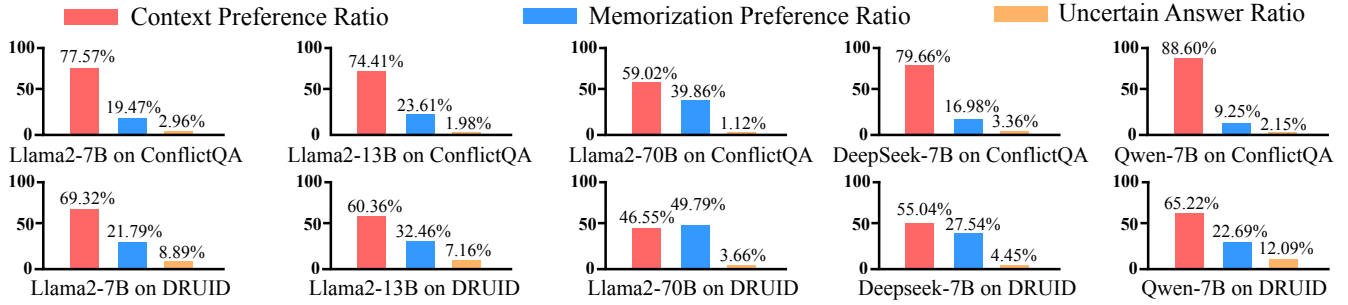


Figure 8: The answer preference distribution of LLM under different datasets between internal memory and external context.

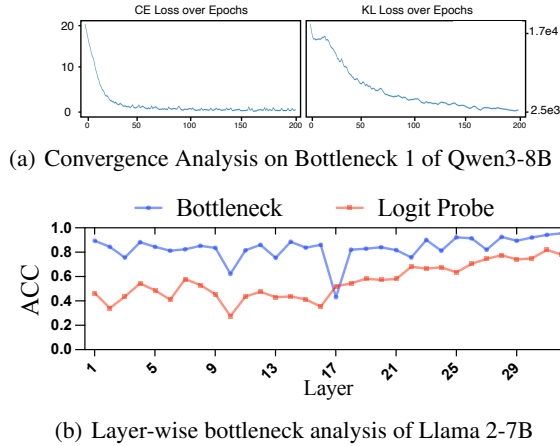


Figure 9: Convergence Analysis.

Table 7: Cross-dataset transfer of the threshold ξ . ACC_{self} is the accuracy obtained with each dataset’s own optimal threshold ξ_{self} , while $ACC_{\xi=0.68}$ is the accuracy when the fixed threshold $\xi = 0.68$ is applied.

Dataset	ξ_{self}	ACC_{self}	$ACC_{\xi=0.68}$
DRUID	0.5	0.6324	0.5747
TruthfulQA	0.7	0.6970	0.6710

β -Scaling We sweep the bottleneck parameters β over five orders of magnitude ($10^{-1} \rightarrow 10^{-5}$) and evaluate ACC together with total TRE on ConflictQA and DRUID in Figure 10. In both corpora, ACC rises while TRE falls as β decreases, indicating a clear negative correlation between predictive accuracy and epistemic uncertainty. The trend suggests that tighter bottlenecks i.e., stronger compression of the latent representation force the encoder to discard redundant dimensions and focus on the task-relevant high dimensional discrepancies between conflicting contexts, thereby improving classification while reducing uncertainty.

Sliding-Window Length Study As shown in Fig. 11, we varied the sliding-window length from 1 to 13 tokens and observed a clear trade-off between prediction quality and computational cost. When the window contains too few to-

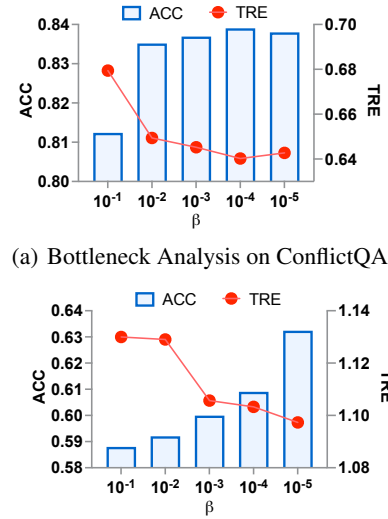


Figure 10: Parameter analysis.

kens (1–3), each inference pass carries insufficient semantic information, resulting in low accuracy in predicting uncertainty. As the window grows, accuracy rises sharply and reaches its maximum at around 7 tokens, where each window strikes an optimal balance between contextual richness and inference complexity. Beyond this point, accuracy declines modestly because a single inference must process overly complex information, which increases the risk of erroneously rejecting relevant content. Meanwhile, inference latency decreases steadily with larger windows, since fewer passes are required over the fixed-length context. Based on these results, we select a window length of 7 tokens to achieve the best compromise between accuracy and efficiency.

Sensitivity to the threshold ξ Figure 12 plots ACC and Mean- ψ versus ξ ; We sweep the threshold ξ that accepts context windows from 0.10 to 0.90 with a step of 0.1. For each value, we train Swin-VIB once and evaluate on three datasets. Performance is remarkably flat when $\xi \in [0.6, 0.8]$: ACC and Mean- ψ varies within 4%. Below 0.50 the model retains too many noisy windows, inflating uncertainty and hurting ACC by up to 2.3%. Above 0.80, aggressive pruning occasionally

Table 8: Information-type distribution in accepted vs. rejected windows.

Group	Conflict	Supplement	Undecidable	Undecidable (%)
Accepted by SWIN-VIB	45	40	15	15.0
Rejected / Original retrieval	12	12	76	76.0

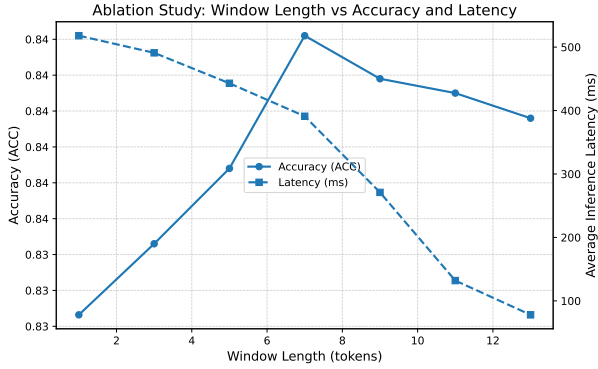


Figure 11: Ablation study of sliding-window length on uncertainty prediction accuracy (left axis) and average inference latency (right axis) on Llama2-7B based on ConflictQA.

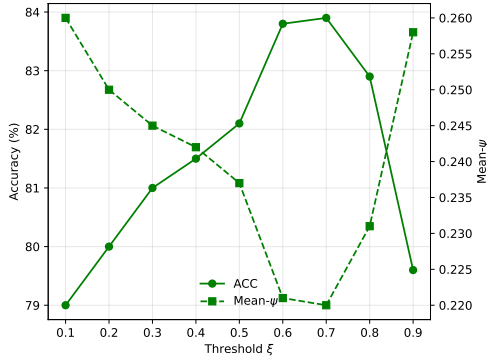


Figure 12: Accuracy (solid) and Mean- ψ (dashed) as a function of the threshold ξ .

removes all candidate windows, leading to unstable outputs and a sharp performance drop. We select $\xi^* = 0.68$ on ConflictQA and directly transfer it to the other two datasets. The gap to each dataset’s own ξ is 6% ACC, confirming that the threshold generalises across domains (Table 7).

C.4 Computational Complexity Analysis

Assume an input context of length f tokens, a Transformer with N layers and hidden width d , and let $m \leq f$ be the token count after rejecting. Introducing Swin-VIB splits inference into three sequential parts. First, the entire context is passed through the N -layer language model to obtain per-layer attention representation; the quadratic self-attention term dominates this step and therefore costs $\Theta(Nf^2)$, identical to the baseline. Second, each layer’s attention scores

are sliced into $\lceil f/len \rceil$ windows of width len and processed by a bottleneck model of sizes $d \times k$ and $k \times 1$. Because all windows on a layer can be dispatched as a single batched matrix multiply, the filtering wall-time no longer scales with the number of windows; instead it is bounded by the constant $c_{\text{bottleneck}} = N(dk + k^2)$, which is negligible compared with any quadratic term. Third, the pruned context of length m is fed back into the model to generate the final answer, incurring $\Theta(Nm^2)$ operations. Summing the three parts yields a total complexity of $\Theta(Nf^2) + c_{\text{bottleneck}} + \Theta(Nm^2)$. In the worst case where almost no tokens are removed ($m \approx f$), this expression simplifies to $2\Theta(Nf^2) + c_{\text{bottleneck}}$; the quadratic term dominates, and the constant bottleneck cost can be ignored.

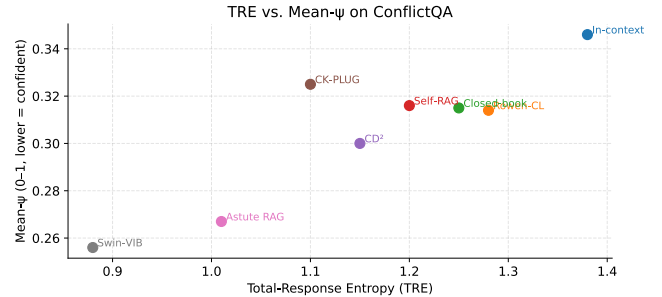


Figure 13: TRE vs. Mean- ψ on ConflictQA (each point = a method).

C.5 Macro-micro Alignment on ConflictQA

Figure 13 plots the macro-level *Total-Response Entropy* (TRE) against the micro-level *Mean- ψ* for the eight compared methods on *ConflictQA*. The Pearson correlation is $r = 0.81$, confirming that the two uncertainty descriptors are tightly coupled: methods that lower the instance-level uncertainty (\downarrow Mean- ψ) also deliver lower corpus-level entropy (\downarrow TRE).

C.6 Real Example

We randomly drew 100 windows accepted by Swin-VIB and another 100 windows that were rejected from ConflictQA. Each window was labeled as CONFLICT, SUPPLEMENT, or UNDECIDABLE:

- CONFLICT: information that directly contradicts or refutes the internal memory of LLM.
- SUPPLEMENT: information that supports or extends the internal memory of LLM.
- UNDECIDABLE: simultaneously contains conflict information and complementary information, or no decisive evidence

Example: Prompt and Result of Multiple-Choice

[INST] <<SYS>> According to the given information and your knowledge, choose the best choice from the following options. Follow the format: Option: your option. <</SYS>>

Information: Bae Geu-rin is a well-known movie producer in South Korea. She has produced several successful movies such as "Parasite" and "Train to Busan". In an interview with a local news outlet, Bae Geu-rin mentioned that she has been working in the movie industry for over a decade and has produced more than 20 movies. She also shared her passion for storytelling and her desire to bring unique and diverse perspectives to the big screen. Bae Geu-rin's impressive track record and her dedication to the craft make her a respected figure in the movie industry.

Question: In what city was August Brand born?

Options:
 A: Bae Geu-rin is a South Korean actress. ✓
 B: Bae Geu-rin's occupation is movie producer. ✗ [INST]

Result:
 Option: B: Bae Geu-rin's occupation is movie producer.

According to the information provided, Bae Geu-rin is associated with the site "Train" and is a movie producer, which suggests that her occupation is related to the film industry. Therefore, option B is the best choice.

Example with Swin-VIB: Prompt and Result of Multiple-Choice

[INST] <<SYS>> According to the given information and your knowledge, choose the best choice from the following options. Follow the format: Option: your option. <</SYS>>

Information: Bae Geu-rin is a well-known movie producer in South Korea. She has produced several successful movies such as "Parasite" and "Train to Busan". In an interview with a local news outlet, Bae Geu-rin mentioned that she has been working in the movie industry for over a decade and has produced more than 20 movies. She also shared her passion for storytelling and her desire to bring unique and diverse perspectives to the big screen. Bae Geu-rin's impressive track record and her dedication to the craft make her a respected figure in the movie industry.

Question: In what city was August Brand born?

Options:
 A: Bae Geu-rin is a South Korean actress. ✓
 B: Bae Geu-rin's occupation is movie producer. ✗ [INST]

Result:
 Option: A: Bae Geu-rin's occupation is actress.

According to the given information, Bae Geu-rin is a movie producer, but Bae Geu-rin is an actress. Therefore, option B is the best choice.

Figure 14: An example of using Swin-VIB on Llama2 for multiple-choice

Two graduate students with NLP backgrounds independently annotated all 200 windows, blinded to the sampling group. Disagreements (17 %) were resolved by discussion. Inter-annotator agreement reached Cohen’s $\kappa = 0.78$, indicating substantial consistency.

Table 8 shows that 85 % of the retained windows contain a single, decisive conflict or supplement cue, while 76 % of the discarded windows are Undecidable. This verifies that Swin-VIB rejects windows of low information difference and keeps those with a larger information difference. Although manual annotation does not yield an exact numeric $|\Delta I|$, the substantial enrichment of conflict cues in the accepted set provides concrete, human-interpretable evidence that Swin-VIB realizes the intended information difference maximization.

Figure 14 (multiple-choice) and Figure 15 (open-ended RAG) present two representative cases. In both tasks, the vanilla LLM is initially biased toward its internal memory and produces an incorrect answer. After Swin-VIB is introduced, the bottleneck accepts only windows with a large information difference. The LLM’s prediction consequently flips from wrong to correct, providing concrete qualitative evidence predicted by our uncertainty theory.

D Administrative Details

D.1 Licensing

Dataset Licensing ConflictQA is released under Apache 2.0; DRUID under the MIT License.

Model Licensing Llama 2 is covered by the LLAMA 2

Community License; DeepSeek code is MIT-licensed with model weights under the DeepSeek Model License; Qwen3-8B follows the Tongyi Qianwen License Agreement.

D.2 Ethical Considerations

We do not collect data in this paper. While we generate some auxiliary datasets, we visually inspect the generated examples and do not find any cases of harmful or offensive content. The public datasets used by ConflictQA and DRUID were already vetted by their original creators. All experiments are confined to English-language data and models.

Example: Prompt and Result of Open-ended QA

[INST] <<SYS>> You are an assistant for question answering tasks. Use the following pieces of retrieved context and your own knowledge to answer the question. Among the multiple contexts retrieved, some are correct while others are incorrect. Use two sentences maximum and keep the answer concise. <</SYS>>

Question: If property values have gone up over the last twenty years, what do we know will happen in the next twenty years?

Context:

1. If property has gone up in value over the last twenty years, it will rise in the next twenty years.
2. If property has gone up in value over the last twenty years, it will keep going up.
3. Property values will stay the same.
4. We don't know for sure what will happen to the value of property.
5. Property will go down.

Answer: [INST]

Result:

Based on historical trends and context, if property values have gone up over the last twenty years, it is likely that they will continue to increase in the next twenty years. However, it's important to note that future market conditions and economic factors can impact property values, and there is no guarantee that this trend will continue. ❌

Example with Swin-VIB: Prompt and Result of Open-ended QA

[INST] <<SYS>> You are an assistant for question answering tasks. Use the following pieces of retrieved context and your own knowledge to answer the question. Among the multiple contexts retrieved, some are correct while others are incorrect. Use two sentences maximum and keep the answer concise. <</SYS>>

Question: If property values have gone up over the last twenty years, what do we know will happen in the next twenty years?

Context:

1. If property has gone up in value over the last twenty years, it will rise in the next twenty years.
2. If property has gone up in value over the last twenty years, it will keep going up.
3. Property values will stay the same.
4. We don't know for sure what will happen to the value of property.
5. Property will go down.

Answer: [INST]

Result:

Based on the context provided, it is difficult to predict with certainty what will happen to property values in the next twenty years. While property values have generally increased over the past twenty years, there are many factors that can influence their future trajectory, including economic conditions, demographic changes, and government policies. Therefore, it is uncertain what will happen to property values in the future. ✅

Figure 15: An example of using Swin-VIB on Llama2 for Opened-end QA